Argon-Photoion–Auger-Electron Coincidence Measurements following *K*-Shell Excitation by Synchrotron Radiation

J. C. Levin, C. Biedermann, N. Keller, L. Liljeby,[a] C.-S. O,[b] R. T. Short,[c] and I. A. Sellin
Department of Physics, University of Tennessee, Knoxville, Tennessee 37996-1200
and Oak Ridge National Laboratory, Oak Ridge, Tennessee 37831-6377

D. W. Lindle
National Institute of Standards and Technology, Gaithersburg, Maryland 20899
(Received 27 April 1990)

Argon photoion spectra have been obtained for the first time in coincidence with *K-LL* and *K-LM* Auger electrons, as a function of photon energy. The simplified charge distributions which result exhibit a much more pronounced photon-energy dependence than do the more complicated noncoincident spectra. In the near-*K*-threshold region, Rydberg shakeoff of *np* levels, populated by resonant excitation of *K* electrons, occurs with significant probability, as do double-Auger processes and recapture of the *K* photoelectron through postcollision interaction.

PACS numbers: 32.80.Dz, 32.80.Hd

The vacancy cascade which fills an inner-shell hole in a single atom is a complex process,[1-8] often leading to a highly charged residual ion. Theoretical modeling of the broad charge distributions resulting from inner-shell photoionization requires understanding many effects, which are often obscured because of the many pathways by which most charge states can be produced. To overcome this limitation, we have measured argon-ion production as a function of photon energy and Auger-decay channel following photoexcitation of *K*-shell electrons by highly monochromatic synchrotron radiation. The advantages of this coincidence requirement, differential in both decay channel and excitation energy, are twofold. First, by requiring that a *K-LL* or *K-LM* Auger electron initiates the vacancy cascade, all primary vacancies are established to be in the *K* shell; otherwise, an initial distribution of *K*, *L*, and *M* vacancies is created. Second, by restricting the first step in the vacancy cascade to a known transition, the resultant photoion charge distribution is greatly simplified. Thus, the photon-energy dependence is rendered more distinct and amenable to interpretation since the ensuing charge distribution is not superimposed on a background of the same charge states produced by different processes with varying thresholds and energy dependences.

Many measurements of noncoincident photoion charge distributions have been made, beginning with experiments conducted long ago by Carlson, Krause, and coworkers using x-ray tubes and filters to photoionize inner shells of neon,[1] argon,[2] krypton,[3] and xenon;[4] the resultant photoions were then analyzed with a magnetic spectrometer. The development of synchrotron radiation sources, with consequent improvement in tunability over x-ray tubes, has resulted in renewed interest in measurements of photoion charge distributions following, e.g., photoionization of the *K* shell of krypton[6] and the *L* and *M* shells of xenon.[7]

Carlson, Krause, and co-workers,[1-4] Tonuma *et al.*,[7] and Mukoyama[8,9] made comparisons of their measurements with results of Monte Carlo simulations of charge distributions. These calculations show general agreement with central features of the broad charge distributions measured, but substantial discrepancies appear, particularly for higher charge states. In addition, the calculations are not applicable to spectra obtained close to threshold.

The experiment was conducted on NIST beam line X-24A at the National Synchrotron Light Source (NSLS) and utilized both multibunch operations (for coincidence measurements) and single-bunch timing mode (for singles measurements). Details of the design[10] and performance[11] of the beam line have been discussed elsewhere. Synchrotron radiation was energy selected, to within ≈ 1 eV, by a double-crystal monochromator [containing Ge(111) crystals], and focused near the tip of a grounded stainless-steel gas jet. The needle was positioned in the extraction region of a time-of-flight (TOF) analyzer, and both were attached to an *XYZ* manipulator which permitted positioning of the needle in the source volume of a commercial cylindrical-mirror electron-energy analyzer. The TOF analyzer consisted of a series of field and drift regions of total length ≈ 5 cm designed both to maintain space focusing and to restrict flight times of argon ions of all charge states to be less than the 550-ns bunch spacing characteristic of NSLS timing-mode operations. Photoions were detected by a pair of chevroned microchannel plates. Care was taken to assure uniform detection efficiency for all charge states; Ar^{q+} ions were accelerated in the last stage of the TOF analyzer to $2.4q$ keV kinetic energy. During timing-mode operations, photoions provided the start signal to a time-to-amplitude convert-

er (TAC) which was stopped by a signal from the storage ring accompanying each burst of photons. In the coincidence measurements, the Auger-electron signal started the TAC, which was then stopped by the photoion signal. To obtain adequate coincidence rates, the cylindrical-mirror analyzer was operated in low-resolution (≈ 20 eV), nonretarding mode. Photoion peak widths were ≈ 2 ns, illustrating the resolution of the TOF spectrometer and associated electronics.

In order to study in detail ion yield as a function of photon energy in the vicinity of the K edge, it was necessary to monitor the energy calibration of the monochromator and to obtain a relative measure of photon flux through the source region. Both were achieved by bracketing each TOF spectrum with an absorption edge obtained by sweeping photon energy across the K edge while recording the total argon-ion yield. The strong peak in the ion signal seen at the $1s$-$4p$ photoexcitation resonance 2.7 eV below the ionization threshold (3206.3 eV) served to calibrate absolute photon energy; all energies in this paper are referenced to this level.[12] The fitted area of this resonance was used to normalize each charge-state intensity to constant flux.

The TOF spectra of Fig. 1 illustrate the simplification in charge distribution which results by requiring a coincidence with each of the three principal Auger lines by which a K vacancy can be filled. Each was obtained with incident radiation tuned to the argon $1s$-$4p$ resonance ≈ 2.7 eV below the K-shell ionization threshold.[12] The broad singles spectrum was obtained in timing mode and represents an average of all possible radiative and nonradiative K-decay channels, with a small superimposed distribution resulting from the decay of less frequently created initial L or M vacancies. Although the Auger spectra are modified by the presence of the $4p$ satellite, diagram-line energies are shifted by only a few eV. The spectra obtained in coincidence with the K-$L_{23}L_{23}$ line at ≈ 2660 eV, K-L_1L_{23} at ≈ 2575 eV, and K-$L_{23}M_{23}$ at ≈ 2923 eV exhibit similarities to each other. Each consists of essentially three peaks; a weak high-charge-state peak, a strong central peak, and a lower-charge-state peak of intermediate intensity (note that Ar^{2+} is produced coincident with K-$L_{23}M_{23}$ but is off scale in Fig. 1). The K-LL coincidence requirement ensures that each ion has two L-shell vacancies; each subsequent Auger or Coster-Kronig decay increases the ion charge by +1. Since L_{23} holes decay in argon with essentially unit probability via L-MM Auger decay,[13] and since L_1 holes decay through L_1-$L_{23}M$ Coster-Kronig transitions with probability 0.94,[13] only the most intense, central "diagram" peak in each coincidence spectrum is expected. The spectra of Fig. 1, obtained 2.7 eV below the K threshold, show richer structure than this simple estimate suggests. Similarly, coincident spectra obtained well above threshold are the result of a number of effects, including energy-dependent shakeoff[14] and ionization of shakeup electrons, and will be discussed in a separate publication.

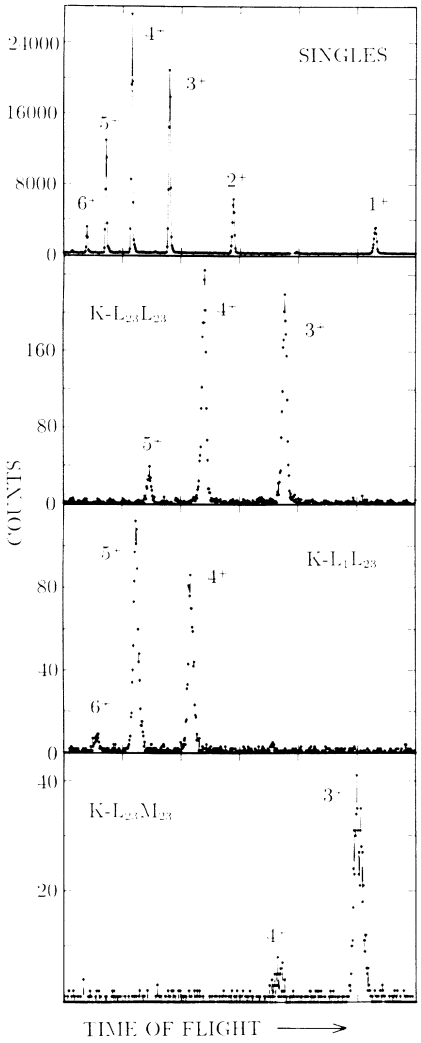

FIG. 1. Time-of-flight spectra for argon photoions produced using synchrotron radiation tuned to the $1s$-$4p$ resonance ≈ 2.7 eV below the K-shell ionization threshold (≈ 3206.3 eV). The last three spectra were measured in coincidence with the indicated Auger line. Although off scale on the bottom spectrum, Ar^{2+} is also produced coincident with K-$L_{23}M_{23}$ electrons, with intensity intermediate to that of Ar^{3+} and Ar^{4+}.

To understand in greater detail the origin of each of the three photoion charges coincident with each Auger electron, we can examine, as a function of photon energy, the intensity of Ar^{3+}, Ar^{4+}, and Ar^{5+}, each normalized to constant photon flux, in the particular case of K-$L_{23}L_{23}$ decay (Fig. 2). All three charge states exhibit a peak at the $1s$-$4p$ resonance; Ar^{3+} has a second peak and shoulder at slightly higher energy before diminishing in intensity to near zero ≈ 10 eV above the resonance. In contrast, Ar^{4+} and Ar^{5+} continue to increase above threshold.

We have simulated the photoion distribution in the

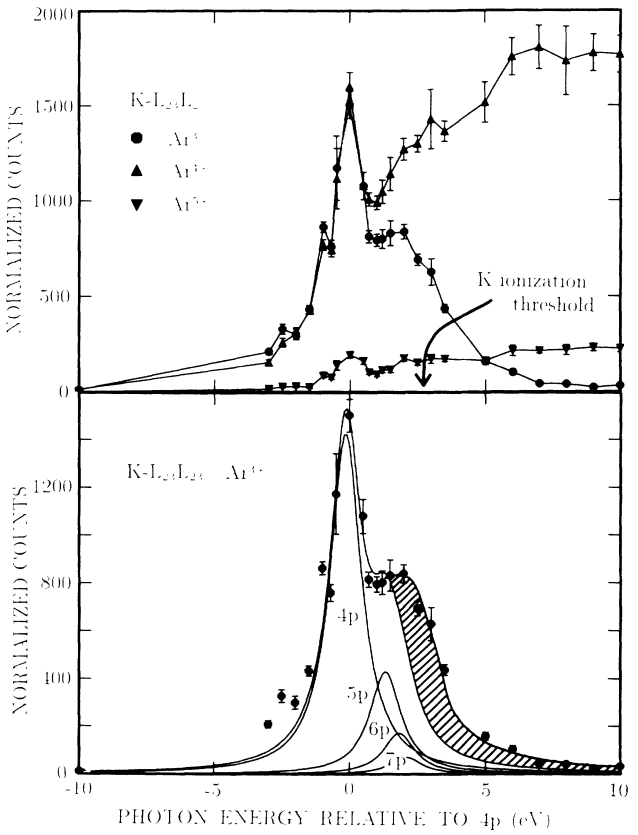

FIG. 2. Top: Argon photoion yields coincident with Ar K-$L_{23}L_{23}$ Auger electrons and normalized to constant photon flux as a function of photon energy relative to the $4p$ resonance. Bottom: Decomposition of Ar^{3+} into components resulting from excitation of the K electron into bound np levels. The shaded area represents recapture of the photoelectron by postcollision interaction.

near-edge energy region by Monte Carlo techniques. Four processes are important: excitation of the K electron to bound np levels, shakeoff of these resonantly populated np levels during subsequent steps in the vacancy cascade, double-Auger processes, and recapture of the K photoelectron above the K edge into bound Rydberg levels via postcollision interaction. We will discuss the contribution of each process to production of Ar^{3+}, Ar^{4+}, and Ar^{5+} coincident with K-$L_{23}L_{23}$ Auger decay.

By analogy to an earlier analysis of an argon absorption edge, we can model the photon-energy dependence of Ar^{3+} in terms of resonant excitation of the K electron to bound np levels (Fig. 2), in which the peak energies have been constrained to be as previously measured.[12] The fitted intensities relative to that of $4p$ ($5p$, 0.30; $6p$, 0.12; $7p$, 0.05) are progressively lower as a function of principal quantum number n than the earlier results ($5p$, 0.37; $6p$, 0.17; $7p$, 0.09).[12] This difference can be ascribed to the greater ease with which electrons in higher Rydberg levels can be ionized during decay of the two L_{23} holes by L-MM Auger decay. Qualitative Monte Carlo simulation of the photoion spectrum in this energy region is consistent with ionization of $\approx (27 \pm 2)\%$ (statistical error) of these resonantly populated np levels during decay of each of the two L_{23} vacancies. We can consider 27% to be a weighted average of ionization from each of the four np levels and assume that these levels are populated initially as measured previously.[12] Using the fitted np intensities (Fig. 2) to provide a measure of fractional ionization from each level, we can estimate ionization probabilities of $4p \approx 19\%$, $5p \approx 34\%$, $6p \approx 43\%$, and $7p \approx 55\%$. We will refer to ionization of electrons in $n \geq 4$ levels by subsequent stages of the vacancy decay as Rydberg shakeoff. In effect, these low-lying Rydberg electrons are removed by shielding changes and/or electron-electron correlation phenomena associated with the departure of an electron in L-MM decay.

In the vicinity of the $4p$ resonance and below, virtually none of the K electrons is excited into the continuum. There are, nonetheless, substantial components of Ar^{4+} and Ar^{5+} produced. Two production mechanisms are responsible. The first is feeding of Ar^{4+} by Ar^{3+} through Rydberg shakeoff of the resonantly populated np levels during one of the subsequent L-MM Auger decays. Since we have seen this to be more likely for the higher-n Rydberg levels, these less tightly bound levels will be preferentially ionized. The result will be an ensemble of Ar^{3+} depleted in the high-n Rydberg component; this is consistent with the deficit in higher-n components observed in the decomposition of Ar^{3+}.

Additional contributions to Ar^{4+} and Ar^{5+} arise from double-Auger (L-MMM) processes, which have been measured to accompany L-MM decay, following L-shell ionization, with probability $(9 \pm 1)\%$.[15] We can estimate the amount of L-MMM decay which occurs following K photoionization from the ratio $Ar^{4+}/Ar^{3+} = (8.1 \pm 0.3)\%$ in the K-$L_{23}M_{23}$ coincident spectra in the photon-energy range 5–15 eV above threshold but below the onset of multielectron processes, which occur 18–35 eV above threshold.[16] Adjusting this ratio for the single missing M-shell electron following K-$L_{23}M_{23}$ decay yields L-MMM/L-$MM = (9.3 \pm 0.3)\%$, in excellent agreement with the earlier result.

About 20 eV above the K-ionization threshold, the Ar^{5+}/Ar^{4+} ratio begins to grow, reaching $\approx 50\%$ several hundred eV above threshold. In the region 10–20 eV above the $4p$ resonance, however, the Ar^{5+}/Ar^{4+} ratio is almost constant at 12%, and can be reproduced by the naive assumption that the two L_{23} decays proceed independently and sequentially and that the first L-MM transition is accompanied by 9.3% L-MMM decay. The second L_{23} decay occurs following partial depletion of the available M-shell electrons by the first L-MM or L-MMM transition. Monte Carlo simulation of the charge distribution, in which this M-shell depletion is included by reducing the L-MMM probability a corresponding amount as the vacancy cascade proceeds, is consistent

with only $L\text{-}MMM/L\text{-}MM=(4\pm1)\%$ for this second decay. Since the double-Auger process is the result of strong correlation among M-shell electrons,[15] this smaller ratio is partly due to the fact that the number of M-shell electron pairs decreases faster than does the number of M electrons. Some contribution to the smaller $L\text{-}MMM$ probability may arise from relaxation of M-shell electrons. The negligible Ar^{6+} signal observed is consistent with low probability of two consecutive $L\text{-}MMM$ decays.

Production of Ar^{4+} is thus seen to occur by different processes in different photon-energy regimes, even in coincidence with a single-Auger process, $K\text{-}L_{23}L_{23}$. Well above threshold, where the K photoelectron has no chance of being recaptured by postcollision interaction, Ar^{4+} follows straightforwardly from $L\text{-}MM$ decay of two L_{23} holes. In the subthreshold energy region, more complicated excitation-autoionization or double-Auger processes are responsible.

There is a clear excess of Ar^{3+} in the photon-energy region 2–7 eV above the $4p$ resonance. At these energies excitation of the K electron into the continuum becomes most probable, with an attendant increase in Ar^{4+} production. The phenomenon of postcollision interaction (PCI), in which the low-energy photoelectron transfers some of its energy to the higher-energy Auger electron, and is itself recaptured into a bound Rydberg level, is responsible for production of Ar^{3+} in this region. This effect has recently been observed in the noncoincident yield of Ar^{+} ions following L photoionization just above threshold[17] and has been explained by a fully quantum-mechanical treatment.[18] The present results show photoelectron recapture extending further above threshold than found previously for the narrower L photoelectron.[17] This is in accord with semiclassical theory in which recapture probability is sensitive to the width of the initial vacancy [$\Gamma_K=0.68$ eV, $\Gamma_L=0.127$ eV (Ref. 19)].

The entire production of Ar^{3+} coincident with $K\text{-}L_{23}L_{23}$ Auger electrons occurs resonantly only in a narrow photon-energy range ≈ 5 eV wide. Neither resonant production nor K-photoelectron recapture by PCI is observed in our noncoincident-photoion spectrum when the K-threshold region is finely probed, again illustrating the power of the coincidence technique used. The effect is obscured in the singles spectrum by the other processes which produce Ar^{3+}.

In this work, we have demonstrated that coincidence measurements of argon photoions with Auger electrons result in charge distributions which are much simpler than previously measured, while permitting study of the photon-energy dependence of phenomena which are not accessible in singles data. Production of different charge states proceeds by quite distinct processes. Below threshold, resonant excitation to bound np levels and frequent Rydberg shakeoff of these levels dominates. Far above threshold, energy-dependent shakeoff and double-Auger effects dominate, and will be discussed in a future publication. At intermediate energies, postcollision interaction provides the bridge resulting in a smooth transition between these regimes.[14]

This work was supported in part by NSF, and by U.S. DOE Contact No. DE-AC05-84OR21400 with Martin Marietta Energy Systems, Inc. Thanks are due Barry Karlin of NSLS, which is supported by U.S. DOE under Contract No. DE-AC020-76CH00016.

[a]Present address: Manne Siegbahn Institute of Physics, S-10405 Stockholm, Sweden.

[b]Present address: Southwestern Medical Center, Dallas, TX 75235.

[c]Present address: Analytical Chemistry Division, Oak Ridge National Laboratory, Oak Ridge, TN 37831.

[1]M. O. Krause, M. L. Vestal, and W. H. Johnston, Phys. Rev. **133**, A385 (1964).

[2]T. A. Carlson and M. O. Krause, Phys. Rev. **137**, A1655 (1965).

[3]M. O. Krause and T. A. Carlson, Phys. Rev. **158**, 18 (1967).

[4]T. A. Carlson, W. E. Hunt, and M. O. Krause, Phys. Rev. **151**, 41 (1966).

[5]T. A. Carlson and C. W. Nestor, Jr., Phys. Rev. A **8**, 2887 (1973).

[6]J. B. Hastings and V. O. Kostroun, Nucl. Instrum. Methods Phys. Res. **208**, 815 (1983).

[7]T. Tonuma *et al.*, J. Phys. B **20**, L31 (1987).

[8]T. Mukoyama, Bull. Inst. Chem. Res., Kyoto Univ. **63**, No. 5-6 (1985).

[9]T. Mukoyama, J. Phys. Soc. Jpn. **55**, 3054 (1986).

[10]P. L. Cowan *et al.*, Nucl. Instrum. Methods Phys. Res. **246**, 154 (1986).

[11]S. Brennan *et al.*, Rev. Sci. Instrum. **60**, 1603 (1989).

[12]M. Breinig *et al.*, Phys. Rev. A **22**, 520 (1980).

[13]M. O. Krause, J. Phys. Chem. Ref. Data **8**, 307 (1979).

[14]G. B. Armen *et al.*, Phys. Rev. Lett. **54**, 182 (1985).

[15]T. A. Carlson and M. O. Krause, Phys. Rev. Lett. **17**, 1079 (1966).

[16]R. D. Deslattes *et al.*, Phys. Rev. A **27**, 923 (1983).

[17]W. Eberhardt *et al.*, Phys. Rev. A **38**, 3808 (1988).

[18]J. Tulkki *et al.*, Phys. Rev. A **41**, 181 (1990).

[19]M. O. Krause and F. H. Oliver, J. Phys. Chem. Ref. Data **8**, 329 (1979).